

**SYSTEMATIC INVERSION OF RECEIVER FUNCTIONS & SURFACE-WAVE DISPERSION FOR
CRUSTAL STRUCTURE IN CENTRAL ASIA**

Charles J. Ammon,¹ George E. Randall,² Jordi Julia,¹ Robert B. Herrmann,³ Eliana Arias,¹ and Theresa Diehl¹

Penn State University,¹ Los Alamos National Laboratory,² Saint Louis University³

Sponsored by National Nuclear Security Administration
Office of Nonproliferation Research and Engineering
Office of Defense Nuclear Nonproliferation

Contract No. DE-FC03-02SF22498

ABSTRACT

We report on our investigations into the seismic structure of the lithosphere in central Asia using surface waves and receiver functions. We are relying on global and regional tomographic analyses for long-period surface-wave dispersion constraints on the structure, which we supplement with short-period observations measured directly from regional signals (when available). We will present an overview of receiver function complexity across the region using results from previous studies and receiver functions from many of the permanent stations. We have completed short-period tomographic imaging of the central and eastern Tibetan Plateau using Love and Rayleigh-waves with periods between 10 and 40 seconds period. The short period information is critical to tight constraints on shallow shear-wave velocity structure, but the measurements are sensitive to source location and origin time uncertainties. We have also surveyed receiver functions from the INDEPTH III experiment and estimated Poisson's ratio variations across the south-central Plateau. We will illustrate the combined inversion of surface-waves and receiver functions using a variety of model constraints focusing on select stations including WMQ, MAK. Our initial efforts have focused on permanent stations and temporary stations for which data are already in hand.

OBJECTIVES

Our objectives are the construction of shear-velocity profiles for regions surrounding broad-band seismic stations throughout central Asia. Application of the technique in the region provides an opportunity to revise models of the crust and upper mantle structure throughout the region and to exploit the global and regional work of previous seismic verification research (*e.g.* Pasyanos et al., 2001; Ritzwoller & Levshin, 1998, Larson and Ekstrom, 2001, Stevens and McLaughlin, 2001). The resulting shear-velocity models provide a single structure consistent with a range of observations and which can be tested as a tool for the construction of mode isolation filters that can help improve surface-wave magnitude estimated. We also plan to explore the possibility of adding additional data to our inversions of receiver functions, surface-wave dispersion. The diverse seismic activity throughout the region will facilitate cross-validation of the mode isolation filters with simple empirical filters constructed using larger events with adequate signal-to-noise ratios.

Background

Much of the background for this project is identical to that found in “Simultaneous Inversion of Receiver Functions, Multi-Mode Dispersion, and Travel-Time Tomography for Lithospheric Structure Beneath the Middle East and North Africa”, by Ammon *et al.*, which appears elsewhere in these proceedings. We refer the reader to this other work for additional background information.

The Joint Inversion of Receiver Functions and Surface-Wave Dispersion Curves

The receiver function is sensitive to velocity transitions and vertical travel times, surface-wave dispersion measurements are sensitive to average-ages of the velocities, and relatively insensitive to sharp velocity contrasts. The complementary nature of the signals makes them ideal selections for joint study because they can fill in resolution gaps of each dataset. Ammon and Zandt (1993) pointed this out in a study of the Landers region of southern California (although for their specific case, available observations were unsuitable to resolve subtle features in the lower crust) and Ozalaybey et al. (1997) and Last et al. (1997) have performed complementary analyses of surface-wave dispersion and receiver functions and Du and Foulger (1999) and Julia et al. (2000) implemented joint inversions of these data types. The mechanics of the inversion are relatively simple since partial derivatives of dispersion observations (Herrmann, 1995) and receiver functions waveforms (*e.g.*, Randall, 1989, Ammon et. al, 1990) can be calculated quickly and accurately. For more details on the method, we refer the reader to Ammon et al. (these Proceedings).

RESEARCH ACCOMPLISHED

Surface-Wave Group-Velocity Imaging of Central Tibet

A critical aspect of constructing an accurate shear-velocity model of the upper crust is the availability of short-period surface-wave observations. Global (Larson and Ekstrom, 2001) and broad regional (Ritzwoller and Levshin, 1998) studies provide very good coverage of the longer period dispersion. In some areas we have relatively closely spaced stations that can allow improvements to these studies on much small scales. Tibet is an area that has drawn much attention due to its tectonic importance. Several field experiments have produced data that can be used to supplement existing studies and improve resolution. As part of our lithospheric imaging efforts, we have combined data recorded within Tibet during the last 13 years for small-to-moderate size earthquakes in an effort to refine group velocity maps of the plateau. Specifically, we gathered waveforms from 190 events located predominantly within the Plateau and recorded on 29 stations that at one time have been deployed within, or immediately adjacent to the Plateau. Although we made measurements for periods from 6 to 45 seconds, periods less than 10 seconds contained sparse measurements and we were not able to perform a useful tomography at these shortest periods.

Sample results for 10 seconds period are shown in Figure 1. To interpret the maps it is necessary to know where the resolution is sufficient. We tested the maximum resolution using checkerboard tests with noise-free numerical “data” computed using the same distribution as the actual observations and inverted using the same smoothness and damping weights that were employed in the inversion. The test results are shown in Figure 2 and indicate that a small

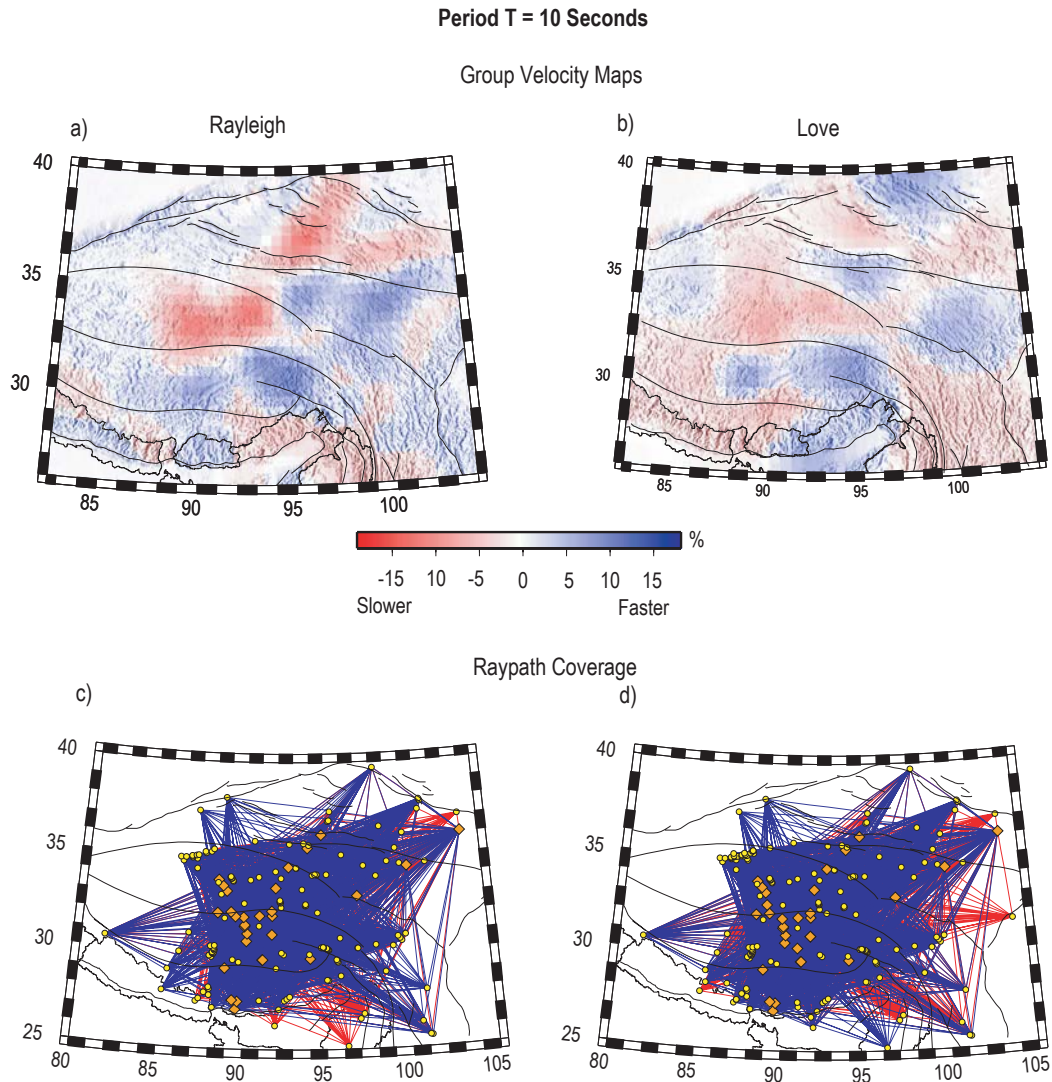


Figure 1. Tomographic results for Rayleigh and Love waves for a period of 10 seconds. The symbols in the lower panels indicate events (yellow circles) and stations (orange diamonds). Not all the stations were operating simultaneously. Paths shown as blue are faster than average, paths shown as red are slower than average.

region near the center of the model is the only area where the spatial resolution is sufficient, although even in the adjacent regions broad averages are constrained by the data. In the region of good resolution, the heterogeneity follows the terrain boundaries. At 10 seconds, the Qiangtang terrain appears to be relatively slow compared with the Lhasa terrain. The boundary between these anomalies nicely follows the suture separating the two terrains.

Our plan is to combine these group velocity information with receiver functions across the region to improve our estimates of the subsurface shear velocity. At present we are experimenting with relocating the events using the group delays to reduce the scatter in the measurements (which is substantial since most paths are short).

Receiver Function Computation

Our focus on receiver function analysis so far is on permanent stations and temporary networks that have completed their monitoring. Data that we have begun to process at the time this report was written are shown in Figure 3. Our

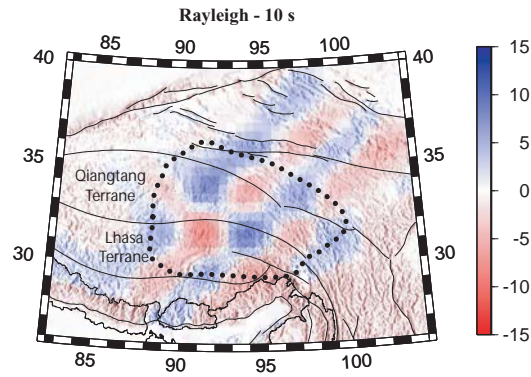


Figure 2. Results of a resolution test for 10-second Rayleigh waves. The target pattern was a checkerboard pattern with $\pm 2.5\%$ slowness variations and a spatial variation of 2.5° . Smoothness prohibits us from recovering sharp features, but the resolution near the center of the model is ideally reasonable. The dotted curve outlines the area of reasonable resolution.

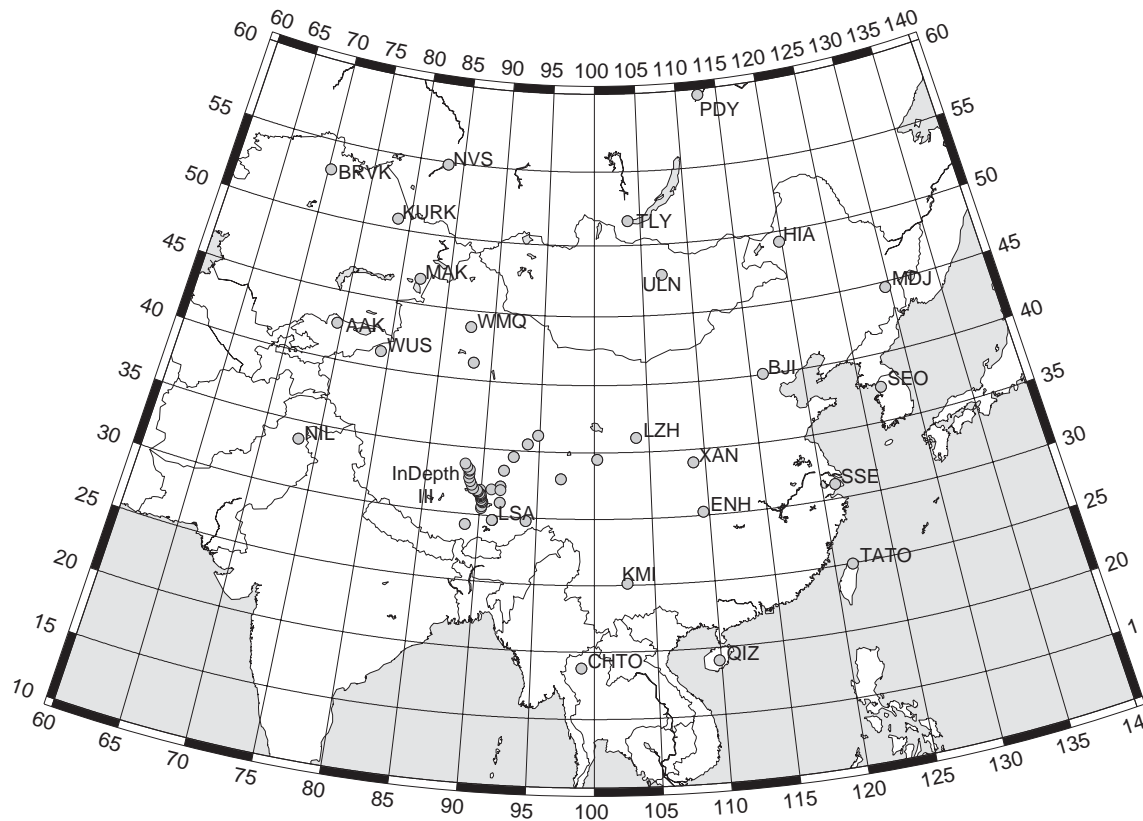


Figure 3. Open stations that we have targeted for analysis as part of this project. The stations are located in a range of environments and most have some regional activity nearby that we can use to add short-period dispersion measurements and to test the resulting shear-velocity models.

approach is relatively simple, we select the station, gather teleseismic P-waveforms for events greater than magnitude 5.5, compute receiver functions using an iterative time-domain approach (Ligorria and Ammon, 1999), and then select the best receiver functions for analysis. Depending on the station, we may cluster the receiver functions as a

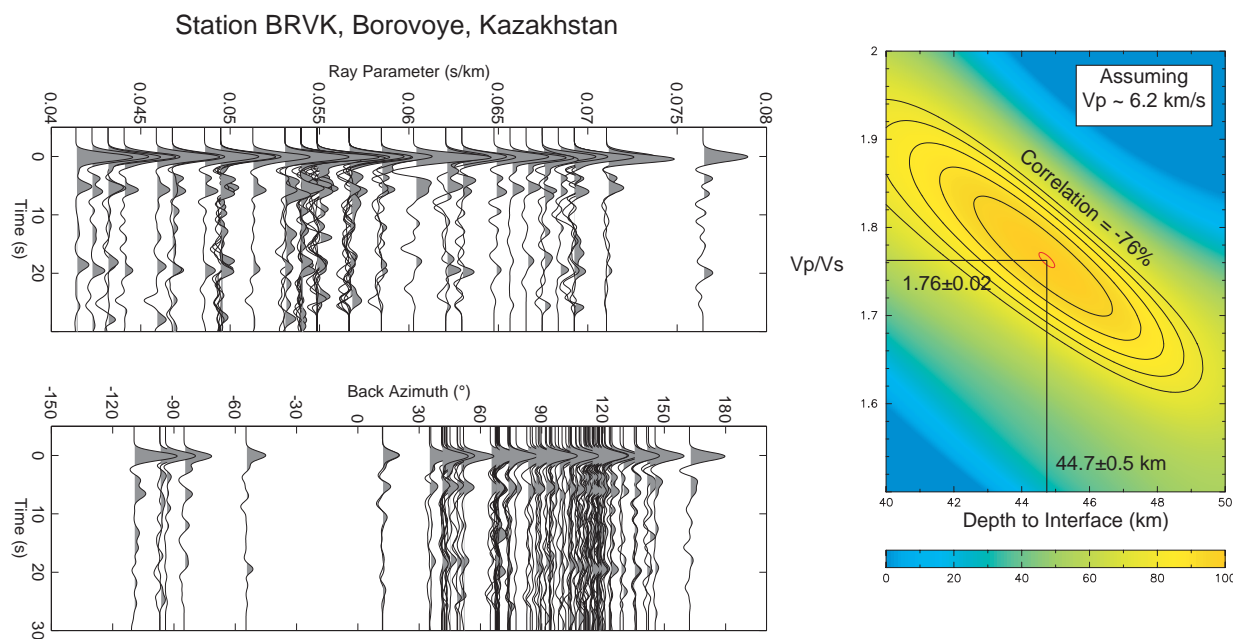


Figure 4. Sample receiver function observations and a limited analysis of Poisson's ratio and crustal thickness (assuming $V_p \sim 6.2$ km/s). The observed receiver functions are shown as a function of ray parameters (\sin of the P-wave incident angle) and as a function of back azimuth. The data do not sample the azimuthal structure uniformly as teleseisms are predominantly observed from western-Pacific subduction zones. The ray parameter sampling is good, and identifiable conversions and multiples are seen clearly for a range of incident angles. The image on the right shows the results of stacking all waveforms to identify the crust-mantle transition. Uncertainties were estimated using a jack-knifing technique. These uncertainties are conservative since they also depend on the assumed P-velocity of the crust. As a result of azimuthal sampling, the results are most reflective of the structure to the east of the station.

function of back azimuth and ray parameter (the amount of data determines the feasibility of this approach). Our analysis usually begins with a relatively simple stacking procedure that allows the estimation of the V_p/V_s ratio (or Poisson's ratio) and crustal thickness (Zhu and Kanamori, 2000). The analysis produces relatively good estimates when the simple assumptions (relatively flat crust-mantle boundary) are satisfied. Example receiver functions for station BRVK in central Asia are shown in Figure 4. Receiver functions generally vary with azimuth and ray parameter and so we summarize our observations in two profiles to show the variation with each. As a first order approximation of the structure, we've ignored azimuthal variation and performed a stacking procedure to use the waveforms to estimate the thickness and Poisson's ratio of the crust (assuming that $V_p \sim 6.2$ km/s) using the method of Zhu and Kanamori (2000). The resulting fits are reasonable, with a thickness value of about 45 km and a Poisson's ratio of 0.26. We will perform similar analyses and inversions for each station with suitable data.

We have examined a subset of the InDepth III broadband seismic profile located in central Tibet (Figure 3). We have estimated receiver functions and performed the waveform stacking procedure to estimate the crustal thickness and Poisson's ratio along the roughly north-south profile (Diehl, 2003). The results from "A" and "B" quality stations are shown in Figure 5. The crustal thickness shows thicker sections to the south, consistent with earlier results. The Poisson's ratio values are more variable and hard to interpret. The complications may be reflective of the relatively simple assumptions of the method which include a relatively flat crust-mantle boundary and isotropy. We have not recovered any evidence that favors a region of high Poisson's ratio between 30.5°N and 32.5°N , which was suggested by Kind et al. (2002). More work is needed to complete the imaging of the entire profile before a final assessment can be made.

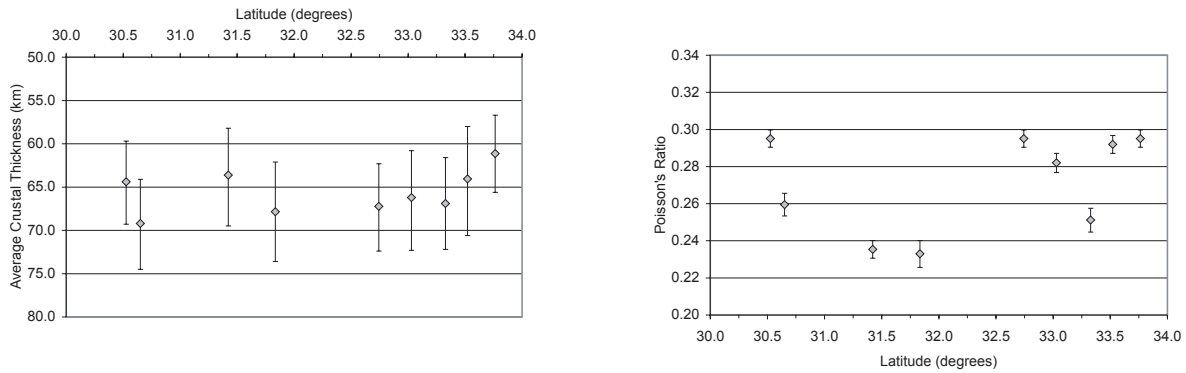


Figure 5. Quality results from an analysis of the inDepth III profile receiver functions using the V_p/V_s crustal thickness tacking method of Zhu and Kanamori (2000). The left panel shows a general thinning of the crust from south-to-north. Poisson's ratio's are more variable. Most of the quality values are between 0.26 and 0.29. The low values near the center of the profile are hard to justify geologically. Our results differ from those of an earlier study.

CONCLUSIONS AND RECOMMENDATIONS

Obviously, our next step is to begin combining our surface-wave and receiver functions into joint shear-velocity inversions. Sharing the group velocity measurements with other groups involved in tomography is also part of our plan, although larger-scale tomographic studies with heavy smoothing may oversimplify the details necessary for imaging variations in shallow crustal structure.

ACKNOWLEDGEMENTS

We thank the P. Wessel and W. H. F. Smith, the authors of GMT for producing easy-to-use, quality software for making maps and charts.

REFERENCES

- Ammon, C.J., G.E. Randall, and G. Zandt (1990), On the non-uniqueness of receiver function inversions, *J. Geophys. Res.*, 95, 15303-15318.
- Ammon, C. J., and G. Zandt (1993), The receiver structure beneath the southern Mojave Block, *Bull. Seism. Soc. Am.*, 83, 737-755.
- Diehl, T. M., Determining Crustal Structure Beneath the Tibetan Plateau Using Receiver Functions, *B. S. Thesis*, Penn State University, University Park, PA, 2003.
- Du, Z.J. and G.R. Foulger (1999), The crustal structure beneath the northwest fjords, Iceland, from receiver functions and surface waves, *Geophys. J. Int.*, 139, 419-432.
- Herrmann, R. B., *Computer Programs in Seismology, 1995*, Saint Louis University, St. Louis, MO, USA.
- Jackson, D.D., Interpretation of inaccurate, insufficient, and inconsistent data (1972), *Geophys. J. R. Astron. Soc.*, 28, 97-109.
- Julia, J., C. J. Ammon, R. B. Herrmann, and A. M. Correig (2000), Joint Inversion of receiver function and surface-wave dispersion observations, *Geophys. J. Int.* 143, 99-112.

25th Seismic Research Review - Nuclear Explosion Monitoring: Building the Knowledge Base

- Kind, R., J. Yuan, J. Saul, D. Nelson, S.V. Sobolev, J. Mechie, W. Zhao, G. Kosarev, J. Ni, U. Achauer, and M. Jiang, Seismic Images of Crust and Upper Mantle Beneath Tibet: Evidence for Eurasian Plate Subduction, *Science*, 298, 1219-1221, 2002.
- Larson, E. W. F. and G. Ekström (2001), Global Models of Group Velocity, *Pure and Applied Geophys.*, 158, 1377-1399.
- Last, R. J., A. A. Nyblade, C. A. Langston and T. J. Owens (1997), Crustal structure of the East African Plateau from receiver functions and Rayleigh wave phase velocities, *J. Geophys. Res.*, 102, 24,469-24,483.
- Ligorria, J.P., and C.J. Ammon, Iterative deconvolution of teleseismic seismograms and receiver function estimation, *Bull. Seism. Soc. Am.*, 89, 1395-1400, 1999.
- Özalaybey, S., M.K. Savage, A.F. Sheehan, J.N. Louie, and J.N. Brune (1997), Shear-wave velocity structure in the northern Basin and Range Province from the combined analysis of receiver functions and surface waves, *Bull. Seismol. Soc. Am.*, 87, 183-199.
- Pasyanos, M.E., W.R. Walter, and S.E. Hazler (2001), A surface wave dispersion study of the Middle East and North Africa for monitoring the Comprehensive Nuclear-Test-Ban Treaty, *Pure and Applied Geophys*, 158, 1445-1474.
- Randall, G. E. (1989), Efficient calculation of differential seismograms for lithospheric receiver functions, *Geophys. J. Int.*, 99, 469-481.
- Ritzwoller, M. H. and A. L. Levshin (1998), Eurasian surface wave tomography: Group velocities, *J. Geophys. Res.*, 103, 1839-1878.
- Stevens, J. L. and K. L. McLaughlin (2001), Optimization of Surface Wave Identification and Measurement, *Pure and Applied Geophys.*, 158, 1547-1582
- Zhu, L., and H. Kanamori (2000), Moho depth variation in Southern California from teleseismic receiver functions, *J. Geophys. Res.*, 105 (2), 2969-2980.